RF SYSTEM DESCRIPTION FOR THE GROUND TEST ACCELERATOR RADIO-FREQUENCY QUADRUPOLE*

Amy H. Regan, Donna Brittain, Daniel E. Rees, and Christopher D. Ziomek
Los Alamos National Laboratory
Los Alamos, NM 87545

Abstract

This paper describes the RF system being used to provide RF power and to control the cavity field for the ground test accelerator (GTA) radio-frequency quadrupole (RFQ). The RF system consists of a low-level RF (LLRF) control system, and RF Reference Generation subsystem, and a tetrode as a high-power amplifier (HPA) that can deliver up to 300 kW of peak power to the RFQ cavity at a 2% duty factor. The LLRF control system implements in-phase and quadrature (I&Q) control to maintain the cavity field within tolerances of 0.5% in amplitude and 0.5° in phase in the presence of beam-induced instabilities.

Figure 1 is a simplified block diagram depicting the major components required to provide a stable RF field inside the accelerating cavity. This paper describes the identified components and presents measured performance data. The user interface with the systems is described, and cavity field measurements are included.

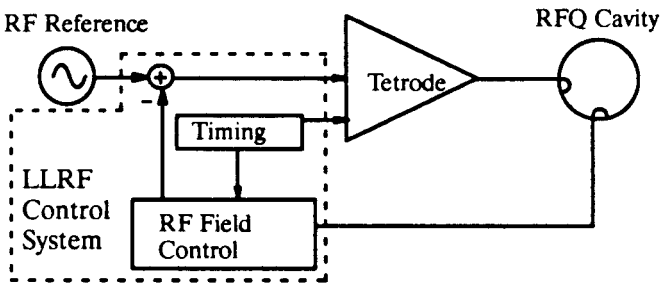

Fig. 1 RF system block diagram.

RF Reference

The RF reference generation subsystem provides coherent, phase-stable signals to each cavity field-control subsystem of the GTA. The reference output signal is low-noise and extremely phase-stable. Figure 2 is a measurement of the RF Reference output spectrum to the LLRF control system.

LLRF Control System

In actuality the LLRF control system performs four separate functions: cavity field control, timing distribution, diagnostic monitoring, and cavity resonance detection. In order to maintain a stable RF field in the cavity, the first two functions are mandatory. These will be discussed.

*Work supported and funded by the US Department of Defense, Army Strategic Defense Command, under the auspices of the US Department of Energy.

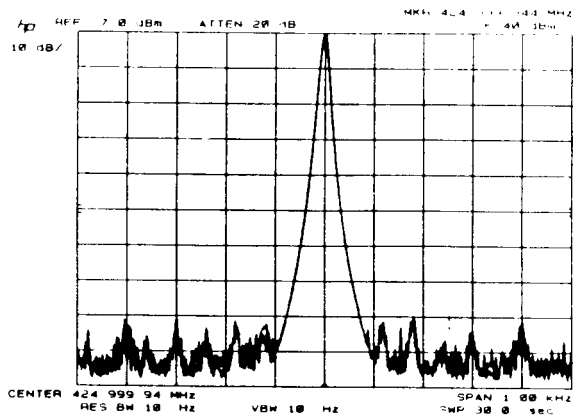

Fig. 2 RF reference spectrum input to feedback loop.

RF Field Control

The field control subsystem regulates the RF field inside the RFQ cavity in the presence of external disturbances by implementing PID-feedback control. This is done by comparing a sample of the accelerating RF field to the input RF reference signal, downconverting this signal to baseband and then resolving it into its in-phase and quadrature components. These I and Q components undergo PID control simultaneously in parallel circuits. The modified components are the control outputs used to modulate the baseband signal. This modulated signal is upconverted to form the LLRF output signal that drives the high-power amplifier. Figure 3 is a functional block diagram of the field control subsystem, whose performance specifications are as follows:

LLRF output (max.)	+ 18 dBm
Steady-state phase error of cavity RF field (max.)	±0.5 elec. degrees
Steady-state amplitude error of cavity RF field (max.)	±0.5%
Response time of LLRF system (max.)	2 μs

The cavity field control system is packaged in the modular VXIbus architecture. Individual VXI modules perform the various functions depicted in Figure 3.

Calibration and setup of the field control subsystem must occur before the accelerator can be operated and whenever accelerator hardware is replaced or modified. Two calibration procedures exist. The first is performed to adjust the phase of the cavity field signal. Due to different electrical lengths of cabling and different devices in the cavity field control subsystem, the cavity field sample has an arbitrary phase rotation. By varying the arbitrary phase shift through the software and observing its effect on test points in the hardware, the phase shift required to produce proper I/Q re-

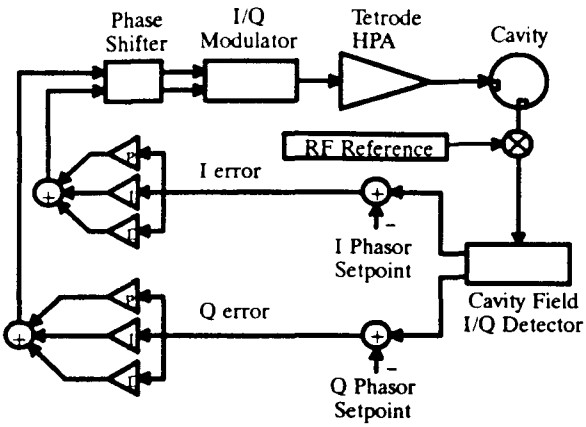

Fig. 3 Functional block diagram of cavity field control system.

lationships is obtained. This phase shift differs with operating setpoint, so a table of proper phase set points is experimentally determined.

The second setup procedure that must take place is the creation of a gain-scheduling table. All of the gains, setpoints, and initial conditions in the control system can be altered by the operator. The gain-schedule table provides data for an interpolation algorithm that automatically calculates these control parameters for any given operating setpoint and is created prior to accelerator operation. This table accounts for any non-linearities within the cavity-fill sequence and within the tetrode amplifier. Creation of the gain-scheduling table requires manual experimentation by an expert user in order to determine proper field control parameters for various operating setpoints. As the parameters are adjusted and determined, the control software enters them into the gain-scheduling table. Again, this procedure involves both interfacing with the hardware through VXI module front panel test points and use of the control software via a workstation.

Timing

The GTA requires synchronous clocks and triggers for the various components of the RF system. These signals are generated within the timing subsystem and are distributed throughout the components. Each field control VXI module incorporates these signals locally, in circuitry based primarily upon the Analog Devices Am9513A system timing controller. The properties of each internal timing signal can be modified through the software. In addition, some modules transmit external timing signals. For example, the HPA RF gate is specified by the operator and is transmitted via a fiber optic cable to the tetrode amplifier. This gate provides an operating window for the HPA driver.

High-Power Tetrode Amplifier

The high-power tetrode amplifier is a three-stage amplifier designed to deliver up to 300 kW of RF power at 425 MHz to the RFQ for 2-ms pulse durations at pulse repetition rates up to 10 Hz. The amplifier consists of an 800-W solid-state driver, which has approximately 45 dB of gain, followed by an air-cooled, 14-kW triode cavity amplifier and a water-cooled Burle 4616 tetrode amplifier, which has a gain of approximately 20 dB and an average anode dissipation of approximately 30 kW. In the GTA application the water-cooled tetrode is operated so that the pulsed saturated output power is approximately 350 kW. However, in short-pulse applications (100 μs), an output of up to 700 kW of peak power has been achieved from the same amplifier architecture with only a 20% change in operating condition and slight cavity modifications. Table 1 includes the operating conditions for the final stage of the tetrode amplifie.

Table 1

Burle 4616 Tetrode Operating Conditions

DC Plate Voltage	19,000 V
DC Screen Voltage	1800 V
Grid Bias	-300 V
DC Plate Current	25.8 A
DC Screen Current	1.0 A
DC Grid Current	.04 A
DC Cathode Current	26.84 A
Fundamental Peak Plate Current	43.3 A
Fundamental Peak Cathode Current	45.3 A
Peak Plate Swing	14,000 V
Peak Grid Swing	300 V
Peak Plate Dissipation	178.1 kW
Peak Screen Dissipation	1800 W
Peak Output Power	300 kW

Figures 4 and 5 represent data taken from some of the latest measurements from the amplifier development for the Superconducting Supercollider. The operating conditions for these measurements differ from those described above in that the anode voltage is 25 kV, the screen voltage is 2200 V, the dc and fundamental current levels are higher due to a higher drive level, and the operating frequency is 427.6 MHz. Figure 4 shows the power transfer characteristic of the amplifier. Note that the input/output characteristics are linear over the range of interest (0-300 kW). This is achieved by operating the first stage class A. The second stage is also operated class A through the use of cathode modulation. The final stage is operated class AB. Figure 5 shows the bandwidth of the amplifier, illustrating a 3-dB bandwidth of approximately 1 MHz at 427.6 MHz.

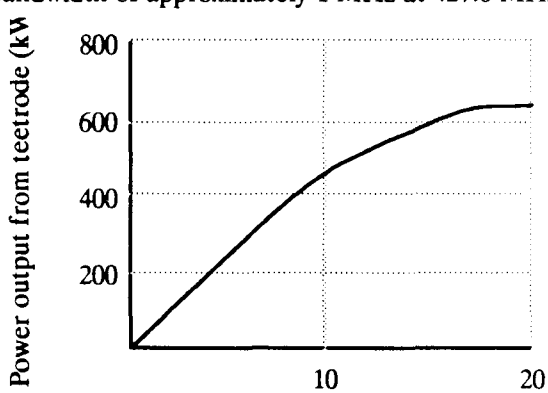

Fig. 4 Amplifier power transfer characteristics.

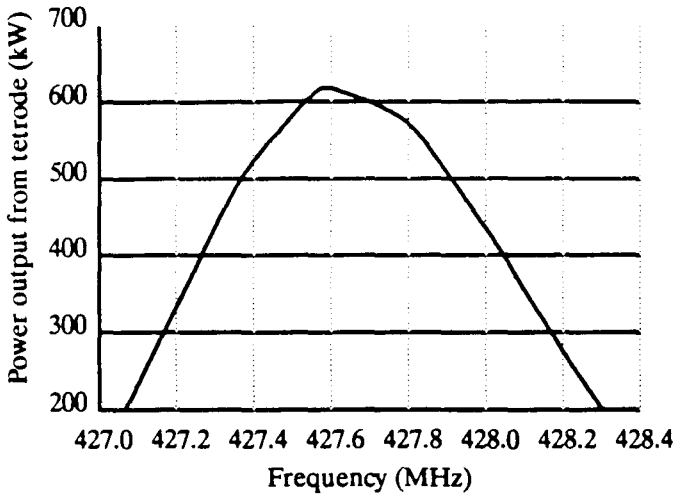

Fig. 5 Amplifier bandwidth.

User Interface

No input from the operator is required for RF Reference during accelerator operation. However, the subsystem does perform self-diagnosis throughout operation and notifies the operator should something fail. For example, the output frequency and power level are constantly monitored and compared to allowable operating ranges. The operator is notified only should these values fall outside of the permissible ranges.

A remote SUN workstation serves as the primary user interface for operating the LLRF and high-power tetrode amplifier systems. The remote operator can turn the systems on/off and control operating parameters. Actual equipment control for the RF subsystems is performed by the local processor resident in each system. Figure 6 shows the relationship between the local area network (LAN) and the RF subsystem processors

The high-power tetrode amplifier system is also locally operable. It is equipped with an Allen Bradley (AB) programmable logic controller, which provides the sequencing of startup, fault and status monitoring, and sequencing of the shutdown of the amplifier equipment. (The user can initiate startup/shutdown of the amplifier system by means of front-panel push buttons when it is in local operating mode.) The local processor is connected through fiber optic cable to a VME-based AB scanner module. The scanner makes portions of the AB processor memory accessible over the VME bus. A VME-based processor and an Ethernet card provide the link to the remote workstation for remote-mode monitoring and operation of the high-power amplifier system.

System Performance Data

When the LLRF, HPA, and control systems were installed and integrated, a series of tests was undertaken to verify that the entire system met the defined specifications. Figures 7 and 8 show measurements of the RFQ RF field I and Q components during operation under closed-loop control with the particle beam present during the pulse. The

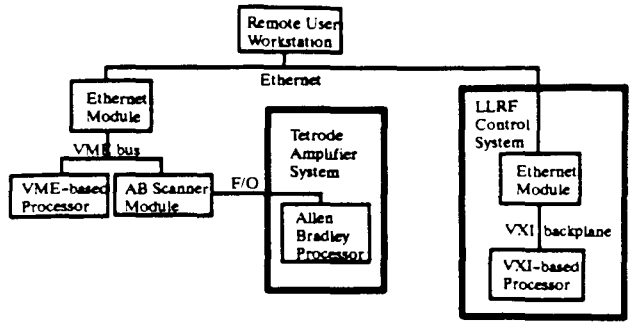

Fig. 6 User interface configuration.

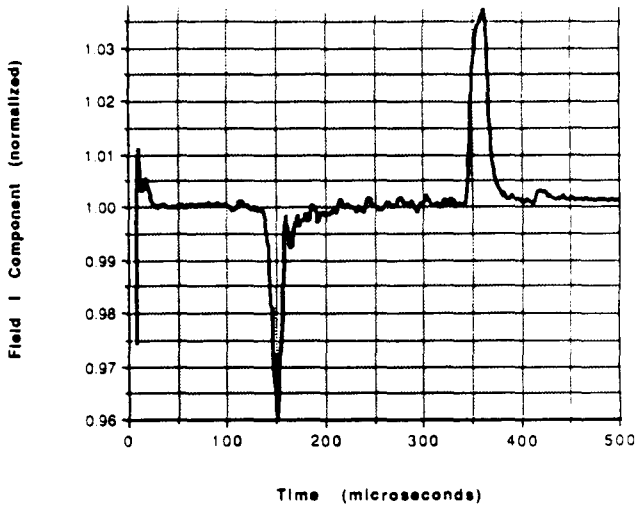

Fig. 7 RFQ cavity field I component during RF pulse.

points where the beam is turned on and off are apparent, as is the level of stability achieved during the beam pulse. The data show performance well-within the 0.5% amplitude and 0.5° phase error budgets.

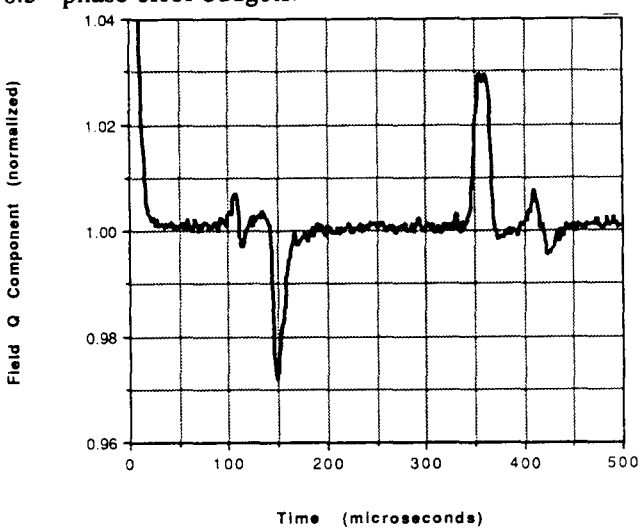

Fig. 8 RFQ cavity field Q component during RF pulse.

Acknowledgments

The authors wish to recognize G.O. Bolme, R. Cole, R. Graybill, D. Kerstiens, S.P. Jachim, J. Power, S. Ruggles, and O.R. Sander for their valuable contributions to this paper.